J Electroceram (2008) 20:127–132
DOI 10.1007/s10832-007-9379-9

Electrical conductivity of the Al-stabilized $La_{2/3}TiO_3$

Ick Soon Kwak · Gyeong Man Choi

Received: 12 July 2007 / Accepted: 22 November 2007 / Published online: 7 December 2007
© Springer Science + Business Media, LLC 2007

Abstract A-site deficient lanthanum titanate ($La_{2/3}TiO_3$) materials with perovskite structure are attractive due to their electrical applications such as ion conductors and dielectrics. However, its stability at room temperature in air is obtained only if Na or Li etc. is incorporated into La site or Al into Ti site. In this study, the electrical conductivities of $La_{0.683}(Ti_{0.95}Al_{0.05})O_3$ have been measured in oxygen partial pressure (Po_2) between 1 and 10^{-18} atm at 1000~1400°C. The electrical conductivity exhibited −1/4, −1/6 and −1/5 dependence ($\log \sigma \propto \log P^n_{O_2}$, n=−1/4, −1/6, −1/5) depending upon temperature and Po_2. The defect model explaining the observation was proposed and discussed. The chemical diffusion coefficient was estimated from the electrical conductivity relaxation.

Keywords La2/3TiO3 · Lanthanum titanate · Electrical conductivity · Defect model · Diffusion coefficient

1 Introduction

Perovskite-related compounds have been extensively studied since they are very interesting materials in the current science and technologies. $La_{2/3}TiO_3$-based compounds with an A-site deficient perovskite-type structure are attractive due to their electrical applications such as ion conductors and dielectrics [1–5]. Pure $La_{2/3}TiO_3$, however, cannot be prepared in air [6] and a mixture of $La_2Ti_2O_7$ and $La_4Ti_9O_{24}$ was obtained during cooling after high temperature sintering [1]. Abe and Uchino prepared $La_{2/3}TiO_{3-\delta}$ perovskite with oxygen nonstoichiometry, δ, ranging from 0.007 to 0.079 under reduced oxygen pressures and examined the crystallographic properties [7]. The structure is of interest since the ordering of cation vacancies and thus superstructure along the c-axis was observed. This compound, however, is not suitable for dielectric use because of its high electrical conductivity due to the Ti^{3+} generated under reducing oxygen pressures [2].

The perovskite structure also was formed by addition of Na or Li to $La_{2/3}TiO_3$ [8]. A-site vacancy concentration decreased with the incorporation of Na or Li into La sites. The Li-added compound obtained was known to show high Li ion conductivity [9]. The partial substitution of Al^{3+} for Ti^{4+} in $La_{2/3}TiO_3$ also decreased the cation vacancy concentration and stabilized the perovskite structure [2]. Among the $La_{(2+x)/3}Ti_{1-x}Al_xO_3$ solid solutions (x=0.05~0.20), the $La_{0.683}(Ti_{0.95}Al_{0.05})O_3$($x$=0.05) material exhibited the highest conductivity.[1] However the detailed electrical properties of the $La_{0.683}(Ti_{0.95}Al_{0.05})O_3$ have not been investigated. The slow equilibration and thus long experimental times required for the Ti-containing compound also make the measurement of electrical conductivity difficult. The addition of $La_{2/3}TiO_3$ into other perovskite material has been used to generate an electronic conductivity at high temperature as shown for the system $[La_{0.9}Sr_{0.1}Al_{0.9}Mg_{0.1}O_3]_{1-x}[La_{2/3}TiO_3]_x$ (x=0–0.30). The mixed p-type and oxygen-ionic conductor, $La_{0.9}Sr_{0.1}Al_{0.9}Mg_{0.1}O_3$, transformed into the mixed n-type and oxygen ion conductor or pure n-type conductor depending upon x ($La_{2/3}TiO_3$ content) at e.g., 1200°C [10].

In this study, we have measured the impedance of $La_{0.683}(Ti_{0.95}Al_{0.05})O_3$ between 400 and 1000°C in air and

I. S. Kwak · G. M. Choi (✉)
Department of Materials Science and Engineering,
Pohang University of Science and Technology,
San 31, Hyoja-dong,
Pohang 790-784, South Korea
e-mail: gmchoi@postech.ac.kr

Present address:
I. S. Kwak
LG Chemical Ltd.,
Daejon, South Korea

thus examined the grain and grain boundary contributions of conductivity. The oxygen partial pressure (Po_2) dependence of electrical conductivity was measured in $10^{-18}<Po_2<1$ atm at 1000~1400°C using four-probe dc technique. The defect model of the material was discussed. From the equilibration kinetics, the chemical diffusion coefficient was also estimated.

2 Experimental

$La_{0.683}Ti_{0.95}Al_{0.05}O_3$ (hereafter LTA05) samples were prepared by solid-state reactions of La_2O_3 (99.9%, Strem Chem., USA), TiO_2 (99.9%, Aldrich, USA) and Al_2O_3 (99.9%, High Purity Chem., Japan) powders. La_2O_3 was pre-fired at 1000°C for 4 h to remove the surface water. Starting powders were weighed and ground with ethanol in an agate mortar. The mixture was calcined at 1300°C for 4 h in air. The calcined powder was reground and then formed into a disc-shape by die pressing, followed by isostatic pressing at 200 Mpa for 5 min and sintered at 1400°C for 8 h in air. The cooling rate was 3 C/min. The phase was identified by X-ray diffraction analysis. Sintered density was measured with the Archimedes method.

Impedance was measured by two-probe method using HP4192a (Yokogawa Hewlett-Packard, Japan) and Solartron 1260 (Schlumberger Technologies, England) at 400~1000°C. The pellet-shaped sample used for the impedance measurement has a dimension of 0.81 cm (diameter)×0.24 cm (thickness). Four-probe dc electrical conductivity, using platinum-paste (Engelhard model No.6926, USA) electrodes, was measured with varying temperature (1000~1400°C) and Po_2 ($1\sim10^{-18}$atm). The rectangular-bar shaped sample had a dimension of 0.22×0.40×0.60 cm. The sample resistance was calculated from the slope of current–voltage curve, obtained by applying current using a current source (Keithley model 220, USA) and measuring a resultant voltage drop using voltmeter (Keithley model 196, USA). The Po_2 values between 1 and 10^{-3} atm and those below 10^{-5} atm, respectively, were controlled by mixing O_2 and Ar gases, and CO and CO_2 gases using mass flow controller. The Po_2 was also checked by a zirconia oxygen sensor. Gas flow rate was maintained at 100 cm^3/min. The electrical conductivity was measured after sample reached an equilibrium, which usually took ~20 h at 1000°C. The Po_2 was subsequently changed to the lower value for the next measurement.

3 Results and discussion

The sintered density of sample was ~98% of theoretical density. X-ray diffraction pattern of LTA05 showed the perovskite having a superstructure with a c-axis doubled (Fig. 1). It is noteworthy that Al^{3+} substitution indeed stabilized the perovskite structure. No second phase was found. Figure 2 shows SEM micrographs of thermally-etched (1300°C/1 h in air) surfaces of LTA05, sintered at 1400°C for 8 h in air. The sample was dense and the grain size was 4.3±0.4 μm as determined using the linear intercept method.

Figure 3 shows a typical impedance pattern for LTA05 measured at 500°C in air. Two semicircles were observed that were easily separated. The frequencies and capacitance values at the peaks of semicircles were indicated and they were 61 kHz and ~2.4×10^{-11} F (relative permittivity, ε_r~126), 12 Hz and ~5×10^{-9} F (effective relative permittivity~2.6×10^4), respectively, for the semicircles located at the high and the low frequencies. Judging from the capacitance values, the grain resistance (R_g) and the grain boundary resistance ($R_{gb}=R_t-R_g$, where R_t is the total resistance), respectively, can be estimated from the high-frequency and the low-frequency intercepts with real axis. The small semicircle for the grain process and the large semicircle for the grain boundary process indicate that the R_g is much smaller than R_{gb}.

Figure 4 shows the temperature dependence of the grain, the grain boundary, and the total conductivity. The grain conductivity obtained in this study ($10^{-4.5}$ S/cm at 700°C) was slightly lower than the reported value ($10^{-4.1}$ S/cm) [1]. The grain conductivity increased with temperature and was smaller than the grain boundary conductivity above ~700°C. Thus the total conductivity was mostly controlled by the grain boundary conductivity below 700°C and by the grain conductivity above 700. At 900°C, the grain boundary conductivity was much higher than that of the grain and thus the measured conductivity at or above 1000°C with four-probe dc technique was assigned as the grain conductivity. Yoshioka and Kikkawa have measured the EMF value of the concentration cell (O_2/air) using LTA05 sample and obtained the ionic transference number of 0.99 at 500°C

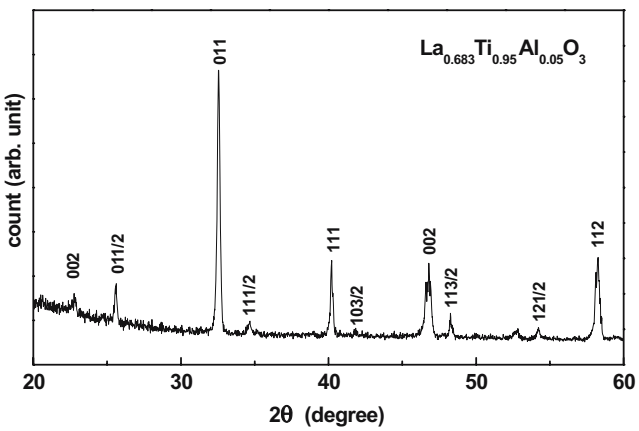

Fig. 1 XRD pattern of LTA05 sintered at 1400°C for 8 h in air

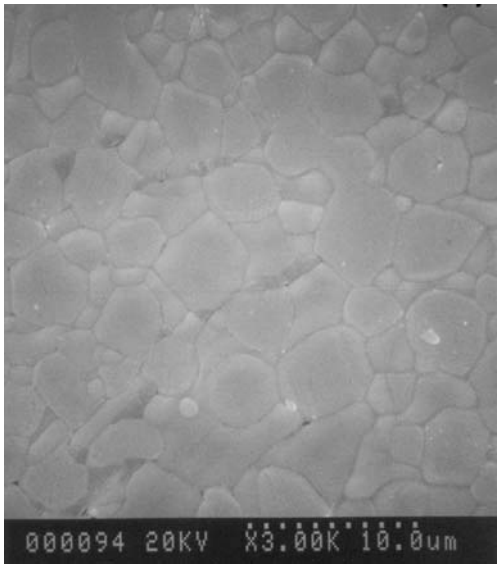

Fig. 2 SEM micrographs of thermally-etched (1300°C/1h in air) surfaces of LTA05, sintered at 1400°C for 8 h in air

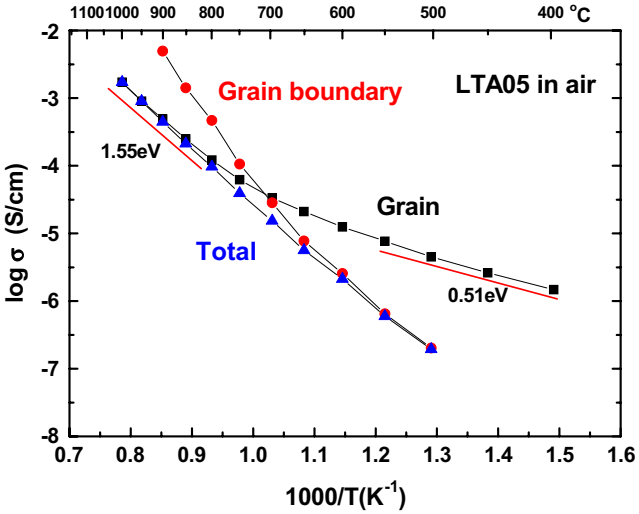

Fig. 4 Temperature dependence of the grain (*square*), the grain boundary (*circle*) and the total (*triangle*) conductivities for LTA05 measured in air. The activation energies of the low temperature and the high temperature grain conductivity were also indicated. Data points are simply connected with lines for visual guide

and 0.62 at 600°C [1]. Thus LTA05 is a predominantly ionic conductor at or blow 500°C and the electronic conductivity increases rapidly with temperature. Assuming a linear change of the ionic transference number with temperature, we expect that the material is an electronic conductor at or above ~800°C. The activation energies of the grain conductivity were 0.51±0.02 eV and 1.55±0.03 eV, respectively, at low temperature (400–550°C) and at high temperature range (800–1000°C). Thus 0.51 eV and 1.55 eV, respectively, are the activation energies of the ionic and the electronic conductivities. It was also shown that the protonic contribution was not shown, judging from the insensitivity of the conductivity to the flowing gases [1].

Figure 5 shows the electrical conductivity, mostly the electronic conductivity due to grain as discussed above, versus Po_2 (1–10^{-18} atm) for LTA05 between 1000 and 1400°C. In a high Po_2 region (>10^{-3} atm), the electrical conductivity exhibited −1/4 slope ($\sigma \propto Po_2^{-1/4}$). In a low Po_2 region (<10^{-4} atm), the slopes were −1/6 or −1/5 depending upon temperature. Numerical values of slopes are shown in Table 1 with Po_2 and temperature. The slopes varying between −1/4 and −1/6 have been found for the Ti-containing compounds such as TiO_2 [11], $BaTiO_3$ [12], and $SrTiO_3$ [13]. The defect model, which is generally used to explain the observed conductivity behavior for the Ti-containing compounds, might be used for the explanation of the current data. At a low temperature (<1200°C) in Po_2 between 10^{-4} and 10^{-12} atm, the observed −1/6 slope can be explained considering the generation of electrons and the

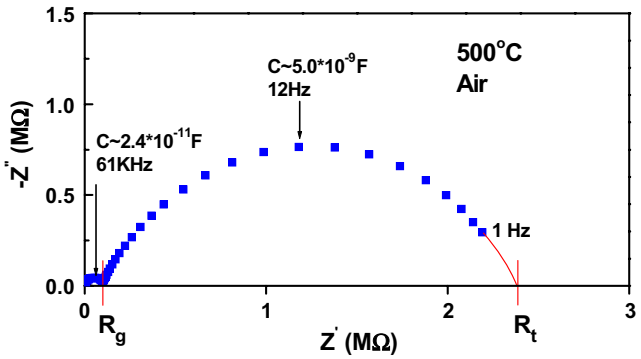

Fig. 3 Impedance patterns of LTA05 measured at 500°C in air. The resistance values (R in Ω) can be transformed into the resistivity values (ρ in Ωcm) ·) by multiplying R with the size factor of the sample [A (Area)/t (thickness)=2.15 cm], i.e., $\rho = R \cdot A/t$)

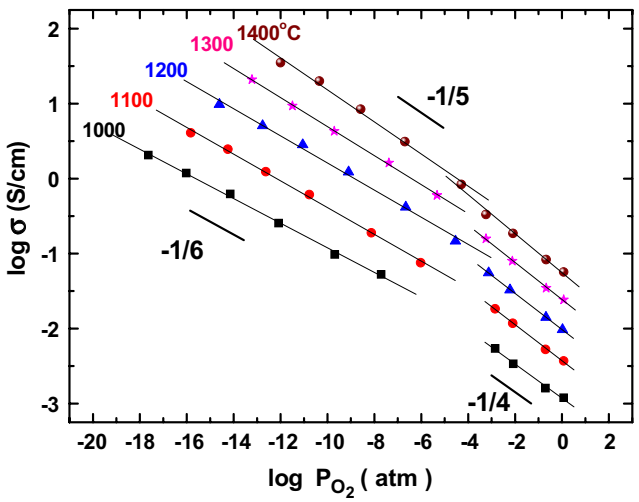

Fig. 5 Electrical conductivity of LTA05 as a function of oxygen partial pressure (1–10^{-18}atm) at 1000–1400°C. *Solid lines* are linear fitting curves. The −1/4, −1/5, and −1/6 slopes are shown for visual guide

Table 1 The experimental values of various slopes (n in $\log \sigma \propto P_{O_2}^{-n}$) of LTA05 at 1000~1400°C.

	High Po_2 (>10^{-4} atm)	Low Po_2 (<10^{-4} atm)
1000°C	1/4.4	1/6.1
1100°C	1/4.2	1/5.6
1200°C	1/4.2	1/5.5
1300°C	1/4.0	1/5.2
1400°C	1/3.9	1/5.0

These slopes were obtained using least square fitting of the data shown in Fig. 5.

doubly-charged oxygen vacancies as a result of the oxygen reduction. The accidental acceptor may generate the additional oxygen vacancies and explains the observed −1/4 slope in $1<Po_2<10^{-3}$ atm region. At high temperature (>1300°C) in low Po_2 (10^{-12}–10^{-4} atm), the −1/5 slope was observed. The transition of slope from −1/4 to −1/6 may explain the −1/5 slope. The generation of other defects may also explain the −1/5 slope. For example, for TiO_2, the −1/5 slope was sometimes explained assuming quadruply-charged Ti interstitial. However, Ti interstitial may not be possible in the perovskite structure. The −1/5 slope is also possible if we assume the co-existence of the singly-charged and the doubly-charged oxygen vacancies.

Figure 6 illustrates the temperature dependence of the electrical conductivity for LTA05 in various Po_2 and Table 2 shows the calculated activation energy. The activation energy was 1.76 eV in pure oxygen atmosphere and increased gradually to 2.33 eV at $Po_2=10^{-12}$ atm. The small activation energy (1.76 and 1.90 eV) was observed in the Po_2 range (1~10^{-3} atm) where −1/4 slope was calculated. According to the defect model discussed above,

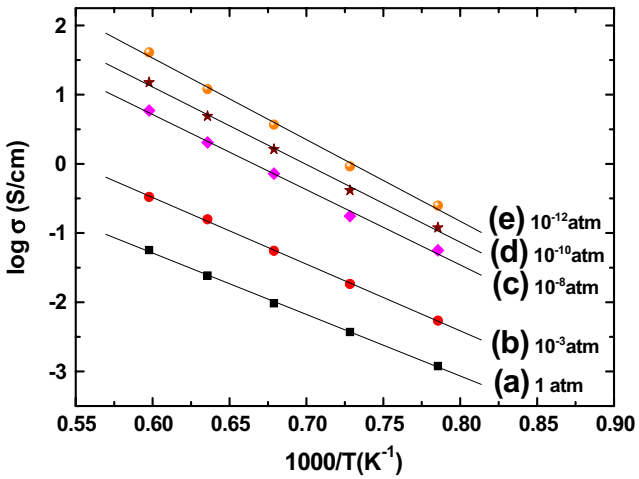

Fig. 6 Temperature dependence of the electrical conductivity for LTA05 with various oxygen partial pressures: (**a**) 1 atm, (**b**) 10^{-3} atm, (**c**) 10^{-8} atm, (**d**) 10^{-10} atm, and (**e**) 10^{-12} atm. *Solid lines* are linear fitting curves

Table 2 Activation energy values of electrical conductivity in a various oxygen partial pressures for LTA05.

Po_2	1 atm	10^{-3} atm	10^{-8} atm	10^{-10} atm	10^{-12} atm
Activation energy (eV)	1.76± 0.03	1.90± 0.03	2.15± 0.07	2.22± 0.07	2.33± 0.08

These values were obtained using the least-square fitting of the data shown in Fig. 6.

the activation energies correspond to $\Delta H_R/2$ in this partial-pressure range, where ΔH_R is the reduction enthalpy oxygen ion, However due to the changing slope from −1/6 to −1/5 with temperature in low Po_2 between 10^{-12} and 10^{-8} atm, the activation energy values were 2.15~2.33 eV.

Figure 7 shows the typical electrical conductivity recorded after oxidation (air→oxygen) and reduction (oxygen→air) with time at 1100°C. In either case, the equilibration took long time (>~7 h), that is often the case for the Ti-containing materials. As can be seen, LTA05 equilibrated after ~50 h during oxidation and ~7 h during reduction. The long equilibration time made the experiment difficult and tedious. The slow equilibration for the other Ti-containing compound is known, for example, for $BaTiO_3$ [14] and $SrTiO_3$ [15] and it was attributed to the slow chemical diffusion. For donor (e.g., Nb)-doped $BaTiO_3$, the slow equilibration (several hours) near 700°C was ascribed to the suppression of oxygen vacancy concentration [14]. On the other hand, the equilibration time of TiO_2 in high Po_2 (>~3 kPa) was ~1 h at 767°C and thus much faster than that of the current LTA05 sample [16]. The fast equilibration was shown for $La_{0.85}Sr_{0.15}MnO_{3-\delta}$, a popular cathode material for solid oxide fuel cell, in Po_2 below 10^{-10} atm [17].

The equilibration time generally depends upon the kinetics of surface exchange and bulk diffusion. The slow equilibration may mean the slow surface-exchange kinetics or the slow bulk diffusion. For the present sample, the reduction was much faster than the oxidation, implying that either the surface-exchange or the chemical diffusion kinetics in the reducing atmosphere is faster than that in the oxidizing atmosphere. For $La_{1-x}Sr_xCo_{1-y}Fe_yO_3$ (LSCF) [18] or $Ba_{1-x}Sr_xCo_{1-y}Fe_yO_3$ (BSCF) [19] materials, both the surface-exchange coefficient (k) and the chemical diffusion coefficient (D_{chem}) decreased with the decreasing oxygen partial pressure (Po_2). On the contrary, for $La_{1-x}Sr_xMnO_3$ (LSM), both the k and the D_{chem} values increased with the decreasing Po_2 [17]. Although the direction of change in the k and the D_{chem} values upon the Po_2 change is different, the k values were proportional to the D_{chem} values for LSCF, BSCF and LSM. The proportionally was also demonstrated for the perovskite materials such as LSM and LSC ($La_{1-x}Sr_xCoO_3$) with empirical relation: $k \propto D_{chem}^{0.5}$ [20]. It was suggested that

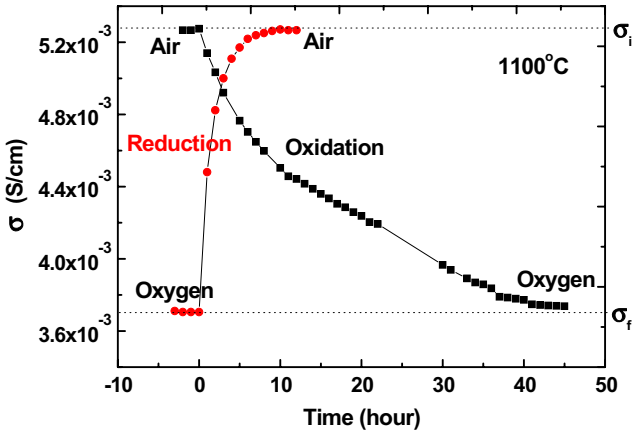

Fig. 7 Typical electrical conductivities for LTA05 recorded during oxidation (air → oxygen) and during reduction (oxygen → air) at 1100°C. Data points are simply connected with lines for visual guide

the vacancy concentration is of prime importance in determining the magnitude of the surface exchange coefficient as well as the diffusion coefficient [20]. With this assumption of the proportionality between k and D_{chem}, the faster equilibration in the reduction process is explained by the higher values of k and D_{chem} in low Po_2 (air) than in high Po_2 (oxygen).

The observed, different equilibration times for the oxidation and reduction are noted. For TiO_2, the equilibrium times for the oxidation (2.8–>55.5 kPa) or the reduction (55.5–>20.6 kPa) were nearly the same [16]. The equilibration times for the reduction and the oxidation were also nearly the same for $La_{0.85}Sr_{0.15}MnO_{3-\delta}$ or $La_{0.6}Sr_{0.4}Co_{1-y}Fe_yO_{3-\delta}$ [17]. The reduction (CO/CO_2 ratio 1/1–>2/1) time was ~1/2 h for $La_{0.85}Sr_{0.15}MnO_{3-\delta}$ at 1000°C [17]. For $La_{0.5}Sr_{0.5}CoO_3$, the conductivity relaxation was much faster during oxidation process than that during reduction process. Substantial differences in the D_{chem} and the k values were found. For the oxidation reaction from 0.01 to 1 atm at 619°C, $D_{chem}=1.49\times10^{-6}$ cm^2/s, and $k=7.40\times10^{-4}$ cm/s, for the reduction reaction from 1 to 0.02 atm, $D_{chem}=1.09\times10^{-6}$ cm^2/s, and $k=1.71\times10^{-4}$ cm/s were found. Thus, ~1.4 times and ~4.3 times higher values were shown for the oxidation reaction than that for the reduction reaction. The difference in the relaxation times between the oxidation and the reduction was attributed mostly to the pressure dependence of the surface exchange reaction [21]. The final Po_2 of the gas switch, irrespective of gas switch direction, determined the kinetics of the conductivity relaxation process [22].

It is not clear which process is the rate limiting process for the present sample between the surface-exchange kinetics and the bulk diffusion. However, for $BaTiO_3$ and $SrTiO_3$, that are two similar Ti-containing perovskite compounds, the chemical diffusion was the rate limiting process as mentioned above. Thus, the D_{chem} value can be estimated from the change in the electrical conductivity with time assuming the surface-exchange kinetics is not rate limiting, following the equation given by Baumard [23];

$$\log\left[1-\frac{\Delta\sigma_t}{\Delta\sigma_k}\right]=\log\left(\frac{512}{\pi^2}\right)-\frac{\pi^2 D_{chem}t}{9.2}\times\left(\frac{1}{a^2}+\frac{1}{b^2}+\frac{1}{c^2}\right) \quad (1)$$

where $\Delta\sigma_k$ is the total change in the conductivity of the sample when the new equilibrium state was established and $\Delta\sigma_t$ is the total change in the conductivity of the sample at time t. The parameters a, b and c are one-half of the each dimension of the sample for the brick-shaped specimen. Eq. 1 requires the following assumptions; that is (1) the mobility of charge carrier is independent of defect concentration and (2) the ionization of defect does not change in the concentration range.

The chemical diffusion coefficient can be determined from the slope of $\log[1-\Delta\sigma_t/\Delta\sigma_k]$ versus time plot as shown in Fig. 8. As can be seen, under oxidizing condition (0.21 → 1 atm) the D_{chem} of LTA05 was $(6.23\pm0.18)\times10^{-8}$ cm^2 s^{-1} and under reducing condition (1 → 0.21 atm) the D_{chem} value was $(5.24\pm0.07)\times10^{-7}$ cm^2 s^{-1}. The D_{chem} value during reduction was ~8 times higher than that during oxidation. The observation may be explained by the difference in the magnitude of the electrical conductivity in reducing and oxidizing condition. The oxygen vacancy concentration is much higher in reducing condition as shown by the high electrical conductivity. Thus, fast equilibration was possible when the sample was exposed to the reducing gas since the sample surface becomes the high diffusivity state.

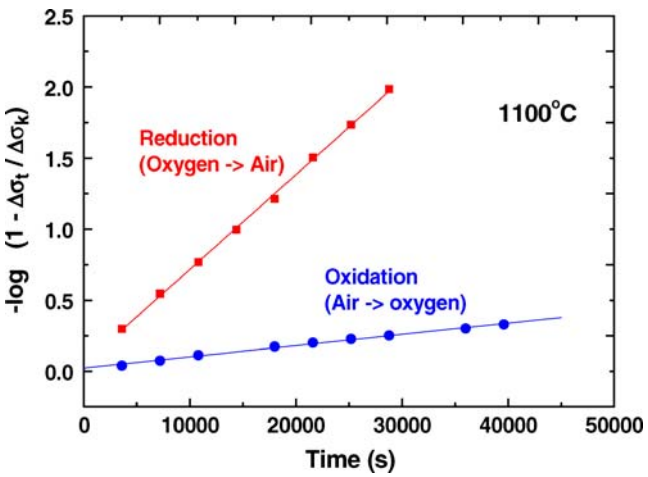

Fig. 8 Logarithmic plots of the electric conductivity change for LTA05. Figure 7 was re-plotted to obtain the kinetic parameter. *Solid lines* are linear fitting curves

4 Conclusions

The electrical conductivity of $La_{0.683}Ti_{0.95}Al_{0.05}O_3$ (LTA05) was measured between 1000 and 1400°C in a wide Po_2 range (1–10^{-18} atm). Under oxidizing condition (1~10^{-3} atm), the electrical conductivity followed the −1/4 slope ($\sigma \propto Po_2^{-1/4}$). Under reducing condition, the electrical conductivity followed the −1/6 or the −1/5 slopes depending upon temperature. The observation was explained by the proposed defect model. The activation energy in oxidizing or reducing atmosphere was estimated. The equilibrium rate of the electrical conductivity under reducing condition was faster than that under oxidation condition. Assuming the surface-exchange kinetics is sufficiently fast, the chemical diffusion coefficient (D_{chem}) of LTA05 was estimated. The D_{chem} for the reduction [$(5.24\pm 0.07)\times10^{-7}$ cm^2 s^{-1}) was ~8 times greater than that for the oxidation [$(6.23\pm0.18)\times10^{-8}$ cm^2 s^{-1}].

References

1. H. Yoshioka, S. Kikkawa, J. Mater. Chem. **8**, 1821(1998)
2. H. Yoshioka, Jpn. J. Appl. Phys. **33**, L945(1994)
3. J. Petzelt, E. Buixaderas, G. Komandin, A.V. Pronin, M. Valant, D. Suvorov, Mater. Sci. Eng. B. **57**, 40(1998)
4. D. Suvorov, M. Valant, S. Skapin, D. Dolar, J. Mater. Sci. **33**, 85 (1998)
5. M. Yokoyama, T. Ota, I. Yamai, J. Crystal Growth **96**, 490(1989)
6. J.B. MacChesney, H.A. Sauer, J. Am. Ceram. Soc. **45**, 416(1962)
7. M. Abe, K. Uchino, Mater. Res. Bull. **9**, 147(1974)
8. A.G. Belous, G.N. Novitskaya, S.V. Polyanetsukaya, Y.I. Gornikov, Izv. Akad. Nauk SSSR, Neorg. Mater. **12**, 470(1987)
9. Y. Inaguma, C. Liquan, M. Itoh, T. Nakamura, T. Uchida, H. Ikuta, M. Wakihara, Sol. St. Comm. **86**, 689(1993)
10. J.Y. Park, G.M. Choi, Sol. St. Ionics **176**, 2807(2005)
11. J. Sasaki, N.L. Peterson, K. Hoshino, J. Phys. Chem. Solids **46**, 1267(1985)
12. N.-H. Chan, R.K. Sharma, D.M. Smyth, J. Am. Ceram. Soc. **64**, 556(1981)
13. G.M. Choi, H.L. Tuller, J. Am. Ceram. Soc. **71**, 201(1988)
14. N.-H. Chan, D.M. Smyth, J. Am. Ceram. Soc. **67**, 285(1984)
15. U. Balachandran, N.G. Eror, J. Electrochem. Soc. **129**, 1021 (1982)
16. M. Radecka, P. Sobas, M. Rekas, Sol. St. Ionics **119**, 55(1999)
17. I. Yasuda, M. Hishinuma, J. Sol. St. Chem. **123**, 82(1996)
18. H.J.M. Bouwmeester, Den Otter, B.A. Boukamp, J Sol. St. Electrochem. **8**, 599(2004)
19. P. Ried, E. Bucher, W. Preis, W. Sitte, P. Holtappels, ECS Trans. **7**, 1217(2007)
20. J.A. Kilner, R.A. De Souza, I.C. Fullarton, Sol. St. Ionics, 86–88 (1996)
21. S. Wang, A. Verma, Y.L. Yang, A.J. Jacobson, B. Abeles, Sol. St. Ionics **140**, 125(2001)
22. J. Yoo, A. Verma, S. Wang, A.J. Jacobson, J. Electrochem.Soc. **152**, A497(2005)
23. J.F. Baumard, Sol. St. Comm. **20**, 859(1976)